Comparison of vascular–function and structure–function correlations in glaucomatous eyes with high myopia

Seung Hyen Lee ,[1] Eun Ji Lee ,[2] Tae-Woo Kim[2]

► Additional material is published online only. To view please visit the journal online (http://dx.doi.org/10.1136/bjophthalmol-2019-314430).

[1]Department of Ophthalmology, Bundang Jesaeng General Hospital, Daejin Medical Center, Gyeonggi-do, Korea (the Republic of)
[2]Department of Ophthalmology, Seoul National University Bundang Hospital, Seoul National University College of Medicine, Seongnam, Korea (the Republic of)

Correspondence to
Dr Eun Ji Lee, Ophthalmology, Seoul National University Bundang Hospital, Seongnam 463-707, Korea (the Republic of); opticdisc@gmail.com

ABSTRACT

Background/aims To determine the usefulness of peripapillary retinal vessel density (VD) measured using optical coherence tomography (OCT) angiography (OCTA) in the evaluation of glaucomatous visual field damage in highly myopic eyes with primary open-angle glaucoma (POAG).

Methods This cross-sectional observational study enrolled a total of 124 myopic POAG eyes consisting of 40 eyes showing a segmentation error (SE) in OCT scans and 84 eyes without an SE. The peripapillary retinal VD, circumpapillary retinal nerve fibre layer thickness (RNFLT) and visual field sensitivity loss (VFSL) were assessed using OCTA, spectral-domain OCT and standard automated perimetry, respectively. The topographical correlations between the VD and VFSL, and between the RNFLT and VFSL were determined in subgroups divided according to the presence of an SE.

Results The peripapillary retinal VD showed significant topographical correlation with VFSL both in the highly myopic POAG eyes without an SE globally (R=0.527, p<0.001), and in temporal (R=0.593), temporal-superior (R=0.543), nasal-inferior (R=0.422) and temporal-inferior sectors (R=0.600, all p<0.001), and in those with an SE globally (R=0.343, p=0.030), and in temporal (R=0.494, p=0.001), temporal-superior (R=0.598, p<0.001), and temporal-inferior sectors (R=0.424, p=0.006). The correlation with VFSL did not differ between the VD and RNFLT in the eyes without an SE

Conclusion Peripapillary VD as measured with OCTA showed a topographical correlation with VFSL in highly myopic POAG eyes regardless of the presence of an OCT SE OCTA may be a useful adjunct for evaluating glaucomatous visual field damage in high myopia, where the OCT results are frequently confounding.

INTRODUCTION

Myopia has been considered a risk factor for the development of glaucoma.[1] The prevalence of myopia is increasing continuously,[2 3] indicating the importance of the diagnosis and treatment of glaucoma in the myopic population. However, precisely evaluating the structural changes associated with glaucoma is challenging in highly myopic eyes due to poor visibility of the retinal nerve fibre layer (RNFL) in red-free photography and the presence of optic disc tilt or an extensive parapapillary atrophy (PPA) preventing an accurate optimal optical coherence tomography (OCT) scanning.[4 5]

OCT angiography (OCTA) is a non-invasive imaging device enabling a quantitative assessment of the peripapillary retinal and choroidal microvasculature.[6–8] Studies have shown that the retinal vessel density (VD) evaluated using OCTA is useful for detecting[6 7] and quantifying[9–11] glaucomatous damage. The retinal VD is lower in glaucomatous eyes than in healthy eyes,[6 7 12] and the magnitude of this decrease in VD is correlated with the severity of the glaucomatous visual field (VF) defect.[9–11] The decreased VD in OCTA images shows an exact topographical correlation with the RNFL defect shown in red-free photography,[13 14] indicating that the retinal VD evaluated using OCTA may accurately reflect structural damage due to glaucoma.

One potential advantage of using OCTA in glaucoma assessments of highly myopic eyes is that it is not affected by the low reflectance of the RNFL or structural deformations of the optic nerve such as optic disc tilt or PPA. Although it is known that retinal VD as measured by OCTA is generally reduced in high myopia,[15 16] it may still be useful to detect microvascular change associated with glaucoma, given the local nature of glaucomatous damage. We hypothesised that the retinal VD obtained using OCTA provides supportive information in case of segmentation error (SE) in the RNFL thickness (RNFLT) measured using OCT. We, therefore, conducted this study to determine the topographical relationship between the retinal VD measured using OCTA and the VF sensitivity loss (VFSL) in highly myopic eyes with primary open-angle glaucoma (POAG), and compared this with the association between RNFLT measured using OCT and VFSL.

METHODS

The participants in this study consisted of POAG patients from the Investigating Glaucoma Progression Study (IGPS), which is an ongoing prospective study that has been underway at the Glaucoma Clinic of Seoul National University Bundang Hospital. Those patients in the IGPS who underwent OCTA imaging of the optic nerve were selected for inclusion in the present study.

Study subjects

A database of subjects included in the IGPS between July 2016 and January 2018 was reviewed. All subjects underwent a complete ophthalmic examination, including visual acuity assessment, refraction, slit-lamp biomicroscopy, gonioscopy, Goldmann applanation tonometry and dilated stereoscopic examination of the optic disc. They also underwent

BMJ

measurements of central corneal thickness (Orbscan II, Bausch & Lomb Surgical, Rochester, New York, USA) and axial length (AXL; IOLMaster V.5, Carl Zeiss Meditec, Dublin, California, USA), stereo disc photography (EOS D60 digital camera, Canon, Utsunomiya-shi, Tochigi-ken, Japan), measurement of the circumpapillary RNFLT using spectral-domain OCT (SD-OCT; Spectralis OCT, Heidelberg, Engineering, Heidelberg, Germany), scanning of the optic disc using OCTA (DRI-OCT Triton, Topcon, Tokyo, Japan), as well as standard automated perimetry (24–2 Swedish interactive threshold algorithm and Humphrey Field Analyzer II 750, Carl Zeiss Meditec).

The untreated intraocular pressure (IOP) was defined as the mean of at least two measurements made before receiving IOP-lowering treatment in the POAG group. The IOP at OCT examination was defined as the IOP at the time when OCTA images were obtained.

Subjects included in the IPGS were required to have a best-corrected visual acuity of at least 20/40. To be included in the present study, subjects were required to be highly myopic, with a spherical refraction ≤6.0 diopters or an AXL >26.0 mm. Eyes that underwent cataract extraction had to conform to the AXL criterion. Those with a history of ocular surgery other than cataract extraction and glaucoma surgery or with other intraocular diseases (eg, age-related macular degeneration, diabetic retinopathy or retinal vessel occlusion) or neurological diseases (eg, pituitary tumours) that could cause VF defects were excluded. Eyes with a history of ocular trauma or uveitis were also excluded.

POAG was defined as the presence of an open iridocorneal angle, signs of glaucomatous optic nerve damage (ie, vertical cup-to-disc ratio ≥0.7, asymmetry ≥0.2 or the presence of neuroretinal rim thinning, notching or a splinter haemorrhage) and associated VF defects without other ocular diseases or conditions that might cause VF abnormalities. A glaucomatous VF defect was defined as (1) values outside the normal limits in the glaucoma hemifield test; (2) 3 abnormal points, with a probability of being normal of $p < 5\%$ and 1 point with a pattern deviation of $p < 1\%$ or (3) a pattern SD of $p < 5\%$. These VF defects were confirmed in two consecutive reliable tests (fixation loss rate ≤20% and false-positive and false-negative error rates ≤25%).

In cases in which both eyes of a subject were eligible for the study, one of the eyes was selected randomly.

Measurement of the RNFLT using SD-OCT

The circumpapillary RNFLT was measured using a circular scanning protocol of the Spectralis OCT system, the details of which are available elsewhere.[17] The diameter of the scan circle spanned 12°, with the diameter in millimetres depending on the AXL. The Spectralis OCT system divides the circumpapillary scanning circle into the following six sectors based on the foveal-disc axis: temporal (T, 316°–45°), temporal-superior (TS, 46°–90°), nasal-superior (NS, 91°–135°), nasal (N, 136°–225°), nasal-inferior (NI, 226°–270°) and temporal-inferior (TI, 271°–315°). The global RNFLT and the RNFLT in each of the six sectors were recorded for analysis. Eyes with poor-quality B-scan images in which the boundary of RNFL could not be identified (ie, quality score <15) were excluded.

The OCT SE was assessed when detecting the RNFL in order to determine whether OCTA could detect glaucomatous damage also in the eyes with improper OCT results (ie, the presence of an SE). An SE was defined as (1) algorithm failure or incorrect segmentation of the anterior or posterior RNFL, (2) incomplete segmentation caused by failure of the algorithm to delineate the

entire extent of the RNFL, (3) cut-edge artefacts due to abrupt lateral edge truncation of the RNFL or (4) pathology-associated artefacts such as PPA.[17] Two independent observers (SHL and EJL) determined the presence of SE. Disagreements between these two observers were resolved by a third adjudicator (T-WK).

Determination of the retinal VD using OCTA

The optic nerve and peripapillary area were imaged using a commercially available swept-source OCTA device (DRI-OCT Triton, Topcon) with a central wavelength of 1050 nm, an acquisition speed of 100 000 A-scans per second, and axial and transversal resolutions of 7 and 20 mm in tissue, respectively. Scans were obtained from 4.5 mm x 4.5 mm cubic areas, with each cube consisting of 320 clusters of 4 repeated B-scans centred on the optic disc. En-face projections of volumetric scans allowed visualisation of the structural and vascular details of various user-defined retinal or choroidal layers. The retinal VD was evaluated in the en-face images segmented in the superficial retina, which were derived from an en-face slab extending from the internal limiting membrane to 130 µm below it. This en-face slab was generated by the DRI-OCT Triton device using automated layer segmentation around the optic nerve head (ONH).

To align the en-face OCTA images to the same orientation as the circumpapillary OCT scans, the OCTA images were superimposed and manually aligned on the infrared fundus image yielded by SD-OCT using ImageJ software (V.1.47, National Institutes of Health, Bethesda, Maryland, USA; available at http://imagej.nih.gov/ij/). The retinal VD was measured using a 750 µm-wide circular annulus extending outward from the outer boundary of the ONH, which was divided into the same six sectors as in circumpapillary OCT scanning: T (316°–45°), TS (46°–90°), NS (91°–135°), N (136°–225°), NI (226°–270°) and TI (271°–315°). The VD was defined as the percentage area occupied by capillaries in the six sectors around the ONH, and it was measured using ImageJ. When the OCTA images were of poor quality, such as due to blurring that hinder the assessment of the vessel contour, the eye was excluded from the analysis. The VD was determined by two independent observers (SHL and EJL), who were blinded to the clinical information of the subjects. The mean of the values was used for the analysis.

Mapping of the RNFLT and retinal VD to VFSL

The topographical relationships of VFSL with the RNFLT and retinal VD were analysed by comparing the RNFLT and retinal VD with the VFSL in each sector (figure 1). The VF total-deviation map was divided into the six sectors using the modified Garway-Heath method proposed by Rao et al.[18] To calculate the mean VFSL in these six regions, the antilog values were calculated at all single test positions and then averaged.[19 20] The average VFSL per sector was converted back to a decibel value for the analysis.[21]

Statistical analysis

The interobserver agreements for determining the presence of an OCT SE and for the measurement of the retinal VD were assessed using kappa statistics (κ value) and the intraclass correlation coefficient (ICC), respectively. Between-group comparisons were performed using Student's t-test for continuous variables and the X^2 test for categorical variables. Correlations of VFSL with the RNFLT and retinal VD were assessed using Pearson's correlation analysis. Bonferroni's correction was applied for multiple comparisons based on the number of sectors within each analysis. Steiger's test was used to evaluate differences in
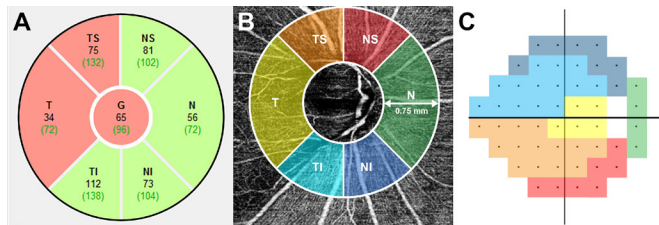
Figure 1 (A) Circular diagram showing the sectoral retinal nerve fibre layer thickness as measured by optical coherence tomography (OCT). (B) En-face OCT angiography (OCTA) image of the superficial retinal layer combined with a diagram of the sectors corresponding to those provided by the Spectralis OCT system (annular radius of 750 µm from the optic disc boundary). (C) Visual field (VF) map divided into sectors using the modified Garway-Heath regions. The sectors in the OCTA image corresponding to the regions in the VF map are depicted in the same colour. G, global; N, nasal; NI, nasal inferior; NS, nasal superior; T, temporal; TI, temporal inferior; TS, temporal superior.

the correlation coefficient between the RNFLT–VFSL and VD–VFSL relationships.

Statistical analyses were performed using the Statistical Package for the Social Sciences (V.22.0, SPSS). Except where stated otherwise, the data are presented as mean±SD values, and a $p < 0.05$ was accepted as significant.

RESULTS
The study initially enrolled 231 POAG eyes of 231 subjects with high myopia, of which 107 eyes were excluded because of poor-quality OCT (n=66) or OCTA images (n=72 eyes). The remaining 124 eyes were further divided into 2 subgroups according to the presence or absence of an SE in detecting the RNFL in OCT circumpapillary RNFL scanning: 40 (32.3%) and 84 eyes (67.7%) were classified as the SE+ and SE− subgroups, respectively. Of the total 40 eyes with SE, 16, 7, 4 and 13 eyes corresponded to the definition (1, 2, 3) and (4), respectively. There was excellent interobserver agreement regarding the determination of the presence of the SE (κ=0.975). The interobserver ICC in measuring the VD was 0.936 (95% CI 0.897 to 0.961).

Baseline characteristics of study subjects
Table 1 describes the demographic and clinical characteristics of the myopic eyes with POAG, and compares between the POAG subgroups with and without an SE Within the POAG group, eyes in the SE+ subgroup had a longer AXL (p<0.001), higher myopic refractive error (p=0.005) and lower VD (p=0.003) than those in the SE− subgroup.

Comparison of the relationships of VD and RNFLT with VFSL according to the presence of SE
Both the global RNFLT and the global retinal VD were significantly correlated with the VFSL (R=0.240 p=0.007 and R=0.470, p<0.001, respectively; table 2). The sectoral analysis revealed a significant correlation between the RNFLT and VFSL in the T, TS, NI and TI sectors (all p≤0.001), and between the retinal VD and VFSL in the T, TS, NS, NI and TI sectors (all p<0.001, table 2). In the SE− subgroup, a significant correlation with VFSL was found for both RNFLT and retinal VD globally and in the T, TS, NI and TI sectors (all p<0.001), with the correlations not differing significantly between the RNFLT and retinal VD (table 2). In the SE+subgroup, retinal VD was correlated with VFSL globally (p=0.030) and in the T, TS and TI sectors (all p≤0.006, table 2). Online supplementary figure 1 shows the linear correlations of average retinal VD and global RNFLT with the VF mean deviation.

Representative cases
Figures 2 and 3 show two POAG eyes with high myopia in the SE+subgroup. The eye in figure 2 had a large PPA inferiorly (figure 2A), and so the OCT circumpapillary scanning circle could not avoid passing through it, resulting in the OCT SE in the inferior sector (figure 2E). Despite the OCT RNFLT measurement not being accurate due to the presence of the SE (figure 2E) and the RNFL defect not being obvious in red-free photography (figure 2B), the en-face OCTA image showed a reduction of the retinal VD in localised area (figure 2C,D) corresponding to the location of the VF defect (figure 2F). Figure 3 shows a POAG eye with high myopia, which is commonly encountered in clinical practice. It was possible to identify glaucomatous damage by confirming the VD decrease (figure 3C,D) corresponding to the VF defect (figure 3F), despite colour and red-free (figure 3A,B)

Table 1	Clinical characteristics			
Variables	POAG (n=124)	SE− group (n=84)	SE+ group (n=40)	P value
Age (years)*	45.5±12.6	44.2±11.0	48.2±15.3	0.105
Gender (male/female)†	78/46	50/34	28/12	0.322
Spherical equivalent (D)*	−8.66±3.16	−8.01±2.47	−10.03±3.96	**0.005**
Axial length (mm)*	27.30±1.39	26.92±0.99	28.11±1.73	**<0.001**
Central corneal thickness (µm)*	539.2±52.5	538.2±46.1	541.2±64.5	0.767
Pretreatment IOP (mm Hg)*	15.5±3.9	15.4±4.3	15.6±3.2	0.821
IOP at examination (mm Hg)*	12.1±2.2	12.0±2.3	12.5±1.9	0.272
VF MD (dB)*	−9.18±5.71	−8.97±6.20	−9.63±4.58	0.508
VF PSD (dB)*	8.79±4.08	8.82±4.36	8.71±3.48	0.880
Global RNFL thickness (µm)*	68.0±21.8	64.7±12.6	72.5±33.8	0.168
OCTA parapapillary vessel density (%)*	53.4±6.0	54.6±5.8	51.1±5.7	**0.003**

Statistically significant values are shown in bold.
*Values are the mean SD unless otherwise specified. P value between subgroups was calculated by Student's t-test.
†P value between subgroups was calculated by the X^2 test.
dB, decibel; D, diopter; IOP, intraocular pressure; MD, mean deviation; OCTA, optical coherence tomography angiography; POAG, primary open-angle glaucoma; PSD, pattern SD; RNFL, retinal nerve fibre layer; SE, segmentation error; VF, visual field.

Table 2 Comparison of correlations between VFSL and RNFLT and between VFSL and vessel density

| | POAG eyes (n=124) | | | | Group A: eyes without SE (n=84) | | | | | | Group B: eyes with SE (n=40) | |
| | RNFLT | | Vessel density | | RNFLT | | Vessel density | | | | Vessel density | |
VFSL	R	P value*	R	P value*	R	P value*	R	P value*	Z score	P value†	R	P value*
VF MD	0.240	**0.007**	0.470	**<0.001**	0.690	**<0.001**	0.527	**<0.001**	−1.577	0.115	0.343	**0.030**
T	0.358	**<0.001**	0.560	**<0.001**	0.528	**<0.001**	0.593	**<0.001**	0.570	0.569	0.494	**0.001**
TS	0.407	**<0.001**	0.575	**<0.001**	0.539	**<0.001**	0.543	**<0.001**	0.034	0.973	0.598	**<0.001**
NS	0.069	0.445	0.386	**<0.001**	0.348	0.009	0.272	0.012	−0.523	0.601	0.397	0.011
N	−0.092	0.310	0.144	0.110	0.172	0.119	0.133	0.227	−0.253	0.801	0.188	0.245
NI	0.299	**0.001**	0.364	**<0.001**	0.480	**<0.001**	0.422	**<0.001**	−0.443	0.658	0.292	0.068
TI	0.526	**<0.001**	0.542	**<0.001**	0.636	**<0.001**	0.600	**<0.001**	−0.351	0.726	0.424	**0.006**

Statistically significant values are shown in bold.

*Bonferroni correction was applied to raw data for measurements in the six sectors. Values that were significant after Bonferroni correction (p<0.0083; 0.05/6) are shown in bold. This was not applied to the global parameters including VF MD, global RNFLT and mean vessel density. Values with p<0.05 were considered significant.

†Comparison of correlation coefficients by Steiger's test.

MD, mean deviation; N, nasal; NI, nasal inferior; NS, nasal superior; POAG, primary open-angle glaucoma; RNFLT, retinal nerve fibre layer; SE, segmentation error; T, temporal; TI, temporal inferior; TS, temporal superior; VF, visual field; VFSL, visual field sensitivity loss.

photography not clearly identifying the presence and location of the damage, and OCT result confounding due to an SE (figure 3E).

DISCUSSION

This study has demonstrated that there is a strong topographical correlation between the peripapillary VD as observed by OCTA and a glaucomatous VF defect in POAG eyes with high myopia. The VD measured using OCTA showed a correlation with VFSL even when it was difficult to detect glaucomatous damage using OCT due to the presence of an SE.

The use of OCT has become widespread during recent decades, and evaluating the peripapillary RNFLT using OCT is now crucial when detecting glaucoma. Considering its importance in clinical practice, the adverse effects of an OCT SE on precise evaluations of the peripapillary RNFLT remains a major concern. The OCT SE occurs more frequently in highly myopic eyes, in which glaucoma develops more frequently than in the non-myopic population.[1 22] There are several explanations for the high frequency of SE in highly myopic eyes. First, axial elongation accompanied by progression of myopia can result in improper alignment of the OCT scan beam, as well as inadequate centreing of the scan circle.[23 24] Second, the large area of PPA beyond the OCT scan circle with a diameter of approximately 3.4 mm would cause an SE and make it difficult to measure the RNFLT accurately. The potential advantage of evaluating the retinal VD using OCTA is that it may be less affected by such an anatomic variation associated with high myopia, because an accurate segmentation may not be as critical for the visualisation of the retinal VD as it may be for the measurement of thickness.

Radial peripapillary capillaries (RPCs) comprise a distinct network of capillary plexus located within the superficial retina that supplies the retinal ganglion cell axons.[25–27] Structural changes to RPCs have been implicated in the pathogenesis of glaucoma.[28] Studies using OCTA have demonstrated a significant association of the VD in the superficial retina (including RPCs) with glaucoma in both functional[29] and structural[30] tests. There is no definite explanation for the causal relationship between the decreased VD in the superficial retina and glaucomatous damage. However, the findings indicate that evaluation of the VD using OCTA may be useful in assessing glaucomatous damage.

Shin *et al*[12] reported that the regional correlation was stronger between the retinal VD and VF mean sensitivity than between the RNFLT and VF mean sensitivity in glaucoma patients with high myopia. However, the present study—which included only highly myopic eyes—did not find that the retinal VD was superior to the RNFLT in the correlation with VFSL in the SE− subgroup. This difference between these studies may be
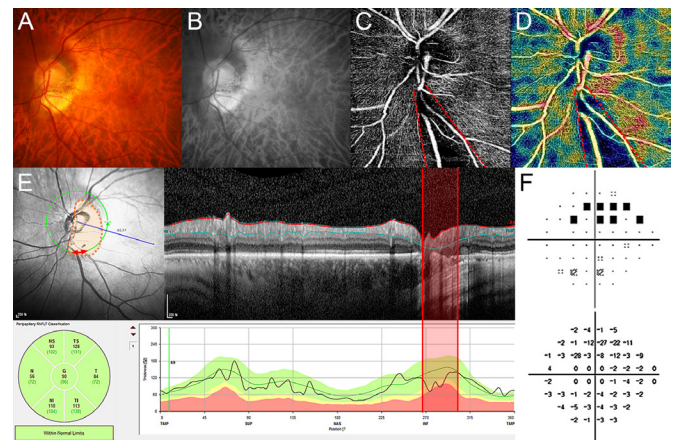

Figure 2 Colour and red-free fundus images (A, B), en-face optical coherence tomography (OCT) angiography (OCTA) images of the superficial retina and that combined with topography of the vessel density (VD) (C, D), OCT circumpapillary retinal nerve fibre layer (RNFL) scan (E) and visual field (VF) pattern-deviation map (F) of a 62-year-old primary open-angle glaucoma patient with high myopia. Dotted lines (C, D) indicate the margins of the area with decreased VD, and double headed arrow and red lines (E) indicate the locations corresponding to those margins. Note that OCTA shows a clearly demarcated wedge-shaped area with decreased VD simulating an RNFL defect (dotted lines, C, D), which topographically corresponds to the location of the VF defect (F). The RNFL defect is not evident either in the colour or in the red-free fundus images (A, B). OCT circumpapillary scanning (green circle) fails to accurately segment the RNFL due to the large area of parapapillary atrophy inferiorly (orange dotted circle), resulting in the inaccurate RNFL thickness measurement (E). G, global; N, nasal; NI, nasal inferior; NS, nasal superior; T, temporal; TI, temporal inferior; TS, temporal superior.
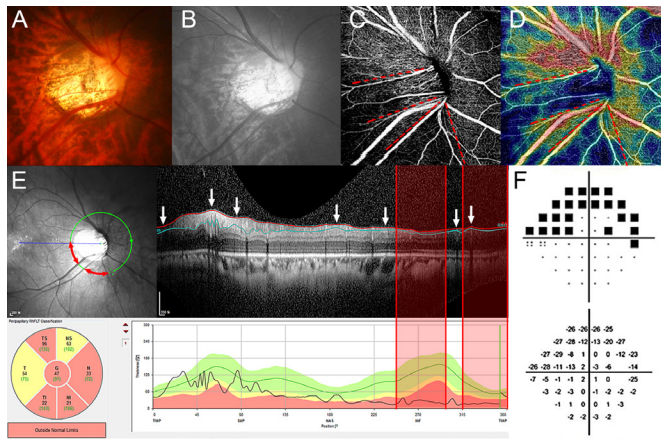
Figure 3 Colour and red-free fundus images (A, B), en-face optical coherence tomography (OCT) angiography (OCTA) image of the superficial retina and that combined with topography of the vessel density (VD) (C, D), OCT circumpapillary retinal nerve fibre layer (RNFL) scan (E) and visual field (VF) pattern-deviation map (F) of a 41-year-old primary open-angle glaucoma patient with high myopia. Dotted lines (C, D) indicate the margins of the area with decreased VD, and double headed arrows and red lines (E) indicate the locations corresponding to those margins. Note that OCTA shows a clearly demarcated wedge-shaped area with decreased VD simulating an RNFL defect (dotted lines, C, D), which topographically corresponds to the location of the VF defect (F). The RNFL defect is not evident either in the colour or in the red-free images (A, B). OCT circular diagram shows abnormal colour codes in all sectors that resulted from segmentation errors in detecting the RNFL (E). G, global; N, nasal; NI, nasal inferior; NS, nasal superior; T, temporal; TI, temporal inferior; TS, temporal superior.

attributable to the different OCT devices used. The Spectralis OCT system has a wider dynamic range than the Cirrus OCT (Carl Zeiss Meditec) system when measuring the RNFLT.[31] It has been shown that the RNFLT measured using the Spectralis system is more strongly correlated with VF sensitivity in eyes with a lower VF sensitivity.[31] Given that RNFL is generally thinner and VF sensitivity is generally lower in highly myopic eyes, the Spectralis OCT system might have detected VF damage more accurately than the Cirrus OCT system. On the other hand, an SE is more readily identified using the Spectralis OCT system, because it provides high-quality B-scan images that the Cirrus OCT does not. It is possible that eyes with an SE were not completely excluded in the study of Shin *et al*, which could have weakened the correlation between the RNFLT and VF mean sensitivity in that study.

The correlation coefficients in the present study were smaller than those shown in Shin *et al*'s study.[12] Although we do not have a clear answer, it is possible that differed clinical characteristics of participants (ie, age, degree of myopia and severity of glaucoma) and the different OCTA device used in each study might be a potential cause for the discrepancy between the studies.

The present study was subject to several limitations. First, only eyes with high myopia were included, and as many as 40% of the eyes were excluded from the analysis, due to either a poor peripapillary B-scan or a low-quality OCTA image that did not allow clear visualisation of the retinal microvasculature. Therefore, the results of this study might only be applicable to eyes for which OCT or OCTA images of acceptable quality are available. Second, the retinal VD was evaluated using the same circular area, while not considering the tilted disc size. Therefore, the measured VD may have included PPA, as in the peripapillary

circumpapillary RNFL scan. The VD is likely to be lower for a tilted disc with a large area of PPA,[32] which may hinder a precise evaluation of the VD; this possibility should be considered when evaluating OCTA images. However, because we analysed the VD, RNFLT and VFSL measured in the same area at the same location, bias resulting from this matter might have been negligible. Third, the cross-sectional design of the study prevented an evaluation of the possible confounding impact of various systemic conditions such as blood pressure or systemic medications on the VD.

In conclusion, the retinal VD as measured using OCTA may be useful in the evaluation of glaucomatous VF damage in highly myopic eyes. The performance of the VD was remarkable even when the RNFLT measured using OCT is not reliable due to SE. Given the relatively high incidence of an OCT SE in highly myopic eyes, evaluation of the VD using OCTA may serve as a useful adjunct to other structural tests, and could potentially substitute them when the results from other conventional tests are affected by confusing factors.

ORCID iDs
Seung Hyen Lee http://orcid.org/0000-0003-2189-2821
Eun Ji Lee http://orcid.org/0000-0001-9393-9452

REFERENCES

1. Mitchell P, Hourihan F, Sandbach J, *et al*. The relationship between glaucoma and myopia: the blue Mountains eye study. *Ophthalmology* 1999;106:2010–5.
2. Vitale S, Sperduto RD, Ferris FL. Increased prevalence of myopia in the United States between 1971-1972 and 1999-2004. *Arch Ophthal* 2009;127:1632–9.
3. Holden BA, Fricke TR, Wilson DA, *et al*. Global prevalence of myopia and high myopia and temporal trends from 2000 through 2050. *Ophthalmology* 2016;123:1036–42.
4. Rauscher FM, Sekhon N, Feuer WJ, *et al*. Myopia affects retinal nerve fiber layer measurements as determined by optical coherence tomography. *J Glaucoma* 2009;18:501–5.
5. Law SK, Tamboli DA, Giaconi J. Characterization of retinal nerve fiber layer in nonglaucomatous eyes with tilted discs. *Arch Ophthal* 2010;128:141–2.
6. Jia Y, Morrison JC, Tokayer J, *et al*. Quantitative OCT angiography of optic nerve head blood flow. *Biomed Opt Express* 2012;3:3127–37.
7. Liu L, Jia Y, Takusagawa HL, *et al*. Optical coherence tomography angiography of the peripapillary retina in glaucoma. *JAMA Ophthalmol* 2015;133:1045–52.
8. Ferrara D, Waheed NK, Duker JS. Investigating the choriocapillaris and choroidal vasculature with new optical coherence tomography technologies. *Prog Retin Eye Res* 2016;52:130–55.
9. Rao HL, Pradhan ZS, Weinreb RN, *et al*. Regional comparisons of optical coherence tomography angiography vessel density in primary open-angle glaucoma. *Am J Ophthalmol* 2016;171:75–83.
10. Shin JW, Lee J, Kwon J, *et al*. Regional vascular density–visual field sensitivity relationship in glaucoma according to disease severity. *Br J Ophthalmol* 2017;101:1666–72.

11 Kumar RS, Anegondi N, Chandapura RS, *et al*. Discriminant function of optical coherence tomography angiography to determine disease severity in glaucoma. *Invest. Ophthalmol. Vis. Sci.* 2016;57:6079–88.

12 Shin JW, Kwon J, Lee J, *et al*. Relationship between vessel density and visual field sensitivity in glaucomatous eyes with high myopia. *Br J Ophthalmol* 2018.

13 Lee EJ, Kim S, Hwang S, *et al*. Microvascular compromise develops following nerve fiber layer damage in Normal-Tension glaucoma without choroidal vasculature involvement. *J Glaucoma* 2017;26:216–22.

14 Lee EJ, Lee KM, Lee SH, *et al*. Oct angiography of the peripapillary retina in primary open-angle glaucoma. *Invest. Ophthalmol. Vis. Sci.* 2016;57:6265–70.

15 Al-Sheikh M, Phasukkijwatana N, Dolz-Marco R, *et al*. Quantitative OCT angiography of the retinal microvasculature and the Choriocapillaris in myopic eyes. *Invest. Ophthalmol. Vis. Sci.* 2017;58:2063–9.

16 Milani P, Montesano G, Rossetti L, *et al*. Vessel density, retinal thickness, and choriocapillaris vascular flow in myopic eyes on OCT angiography. *Graefes Arch Clin Exp Ophthalmol* 2018;256:1419–27.

17 Liu Y, Simavli H, Que CJ, *et al*. Patient characteristics associated with artifacts in spectralis optical coherence tomography imaging of the retinal nerve fiber layer in glaucoma. *Am J Ophthalmol* 2015;159:565–76. e2.

18 Rao HL, Zangwill LM, Weinreb RN. Structure-Function relationship in glaucoma using spectral-domain optical coherence tomography. *Arch Ophthal* 2011;129:864–71.

19 Kim J-A, Kim T-W, Lee EJ, *et al*. Microvascular changes in peripapillary and optic nerve head tissues after trabeculectomy in primary open-angle glaucoma. *Invest Ophthalmol Vis Sci* 2018;59:4614–21.

20 Lee EJ, Kim T-W, Kim J-A, *et al*. Parapapillary Deep-Layer microvasculature dropout in primary open-angle glaucoma eyes with a parapapillary γ-Zone. *Invest. Ophthalmol. Vis. Sci.* 2017;58:5673–80.

21 Wu H, de Boer JF, Chen L, *et al*. Correlation of localized glaucomatous visual field defects and spectral domain optical coherence tomography retinal nerve fiber layer thinning using a modified structure–function map for OCT. *Eye* 2015;29:525–33.

22 Suzuki Y, Iwase A, Araie M, *et al*. Risk factors for open-angle glaucoma in a Japanese PopulationThe Tajimi study. *Ophthalmology* 2006;113:1613–7.

23 Kim T-W, Kim M, Weinreb RN, *et al*. Optic disc change with incipient myopia of childhood. *Ophthalmology* 2012;119:21–6.

24 Hong S, Kim CY, Seong GJ. Adjusted peripapillary retinal nerve fiber layer thickness measurements based on the optic nerve head scan angle. *Invest. Ophthalmol. Vis. Sci.* 2010;51:4067–74.

25 Henkind P. Radial peripapillary capillaries of the retina. I. anatomy: human and comparative. *British Journal of Ophthalmology* 1967;51:115–23.

26 Henkind P, Bellhorn RW, Poll D, *et al*. 3. their development in the cat. *Br J Ophthalmol* 1973;57:595–9.

27 PK Y, Cringle SJ, DY Y. Correlation between the radial peripapillary capillaries and the retinal nerve fibre layer in the normal human retina. *Exp Eye Res* 2014;129:83–92.

28 Kornzweig AL, Eliasoph I, Feldstein M. Selective atrophy of the radial peripapillary capillaries in chronic glaucoma. *Arch Ophthal* 1968;80:696–702.

29 Yarmohammadi A, Zangwill LM, Diniz-Filho A, *et al*. Relationship between optical coherence tomography angiography vessel density and severity of visual field loss in glaucoma. *Ophthalmology* 2016;123:2498–508.

30 Kim SB, Lee EJ, Han JC, *et al*. Comparison of peripapillary vessel density between preperimetric and perimetric glaucoma evaluated by OCT-angiography. *PLoS One* 2017;12:e0184297.

31 Lee KM, Kim T-W, Weinreb RN, *et al*. Anterior lamina cribrosa insertion in primary open-angle glaucoma patients and healthy subjects. *PLoS One* 2014;9:e114935.

32 Akagi T, Iida Y, Nakanishi H, *et al*. Microvascular density in glaucomatous eyes with hemifield visual field defects: an optical coherence tomography angiography study. *Am J Ophthalmol* 2016;168:237–49.